

# Обзор ArXiv/astro-ph, 1-14 марта 2023 года

От Сильченко О.К.

# ArXiv: 2303.00384

## Misaligned gas accretion as a formation pathway of S0 galaxies

Yuren Zhou,<sup>1,2,3</sup> Yanmei Chen,<sup>1,2,3</sup>★ Yong Shi,<sup>1,2,3</sup> Qiusheng Gu,<sup>1,2,3</sup>

Junfeng Wang,<sup>4</sup> and Dmitry Bizyaev,<sup>5,6</sup>

<sup>1</sup>*School of Astronomy and Space Science, Nanjing University, Nanjing 210093, China*

<sup>2</sup>*Key Laboratory of Modern Astronomy and Astrophysics (Nanjing University), Ministry of Education, Nanjing 210093, China*

<sup>3</sup>*Collaborative Innovation Center of Modern Astronomy and Space Exploration, Nanjing 210093, China*

<sup>4</sup>*Department of Astronomy and Institute of Theoretical Physics and Astrophysics, Xiamen University, Xiamen, Fujian 361005, China*

<sup>5</sup>*Apache Point Observatory and New Mexico State University, PO Box 59, Sunspot, NM 88349-0059, USA*

<sup>6</sup>*Sternberg Astronomical Institute, Moscow State University, Moscow 119992, Russia*

Accepted XXX. Received YYY; in original form ZZZ

### ABSTRACT

We select 753 S0 galaxies from the internal Product Launch-10 of MaNGA survey (MPL-10) and find that  $\sim 11\%$  of S0 galaxies show gas-star kinematic misalignments, which is higher than the misaligned fraction in spiral ( $\sim 1\%$ ) and elliptical galaxies ( $\sim 6\%$ ) in MPL-10. If we only consider the emission-line galaxies (401 emission-line S0s), the misaligned fraction in S0s increases to  $\sim 20\%$ . In S0s, the kinematic misalignments are more common than the merger remnant features ( $\sim 8\%$ ). Misaligned S0s have lower masses of stellar components and dark matter halos than S0s with merger remnant features. Based on the  $NUV - r$  versus  $M_*$  diagram, we split galaxies into three populations: blue cloud (BC), green valley (GV) and red sequence, finding that BC and GV misaligned S0s have positive  $D_n4000$  radial gradients which indicates younger stellar population in the central region than the outskirts. Through comparing the misaligned S0s with a control sample for the whole S0 galaxy sample, we find that the BC and GV misaligned S0s show younger stellar population at  $R \lesssim R_e$  and older population at  $R \gtrsim R_e$  than the control samples. Considering the high incidence of kinematic misalignments in S0 galaxies and the properties of environments and stellar populations, we propose misaligned gas accretion as an important formation pathway for S0s.

**Key words:** galaxies: formation – galaxies: kinematics and dynamics – galaxies: elliptical and lenticular, cD

# MaNGA: S0s – отдельно с газом misaligned, отдельно с признаками взаимодействия

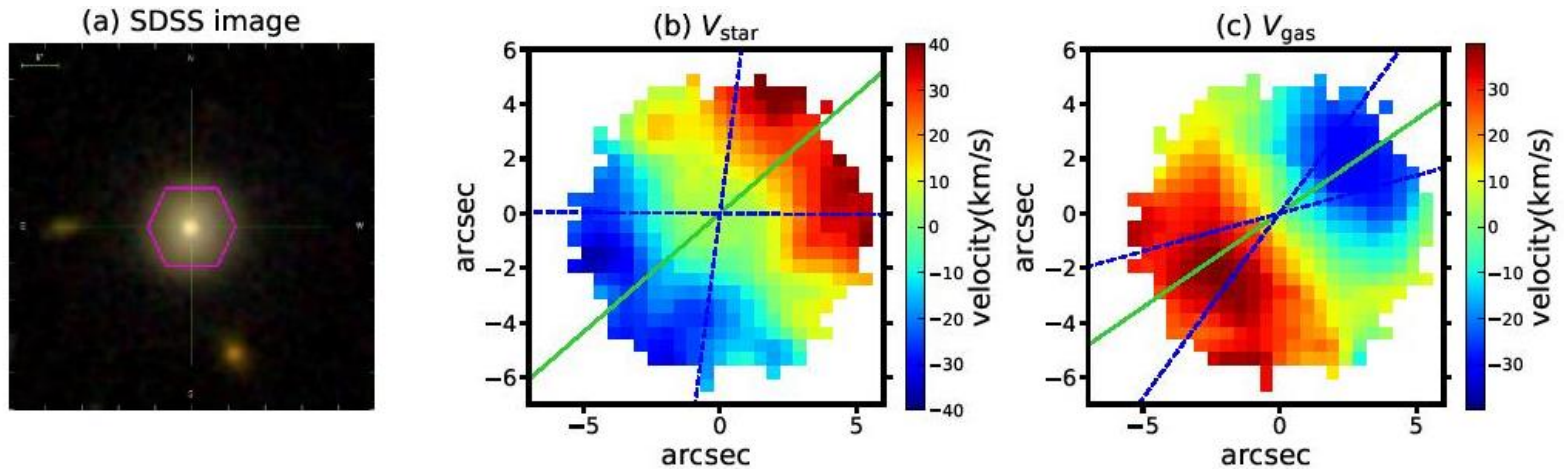


**Figure 1.** An example of misaligned S0 galaxy. Panel (a) displays the SDSS  $g$ ,  $r$ ,  $i$ -band images with the purple hexagons marking the MaNGA bundle. Panel (b) and (c) show the velocity fields for the stellar and gaseous (traced by  $H\alpha$ ) components, respectively. The red side moves away from us while the blue side moves towards us. The green solid line mark the position angle (PA) of kinematic major axis with blue dashed lines being  $\pm 1 \sigma$  errors of PAs.

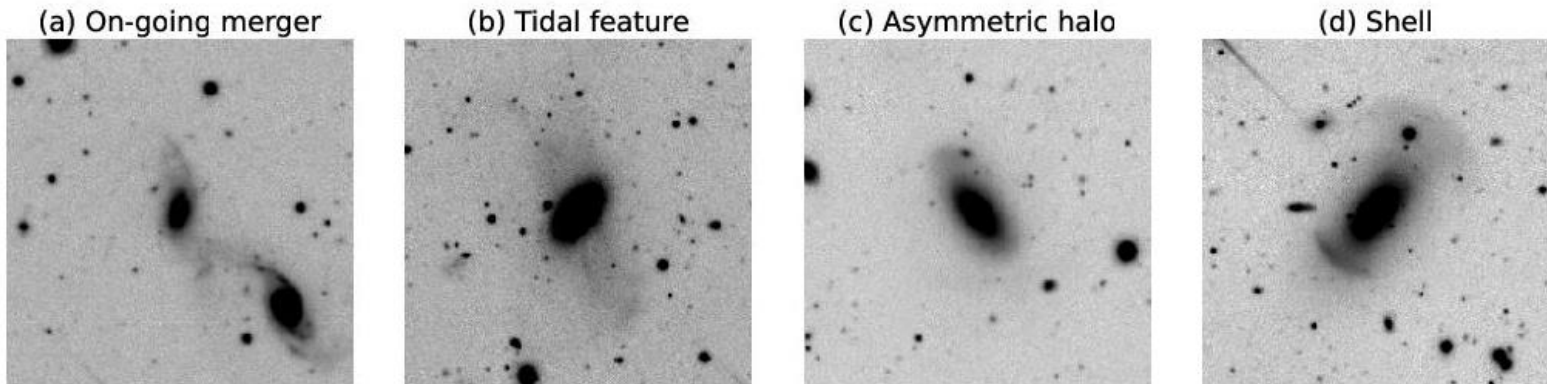


**Figure 2.** Classification of galaxies with interacting features: (a) on-going merger; (b) a galaxy with tidal features; (c) a galaxy with extended asymmetric stellar halo; (d) a galaxy with shell.

# В основном – красная последовательность

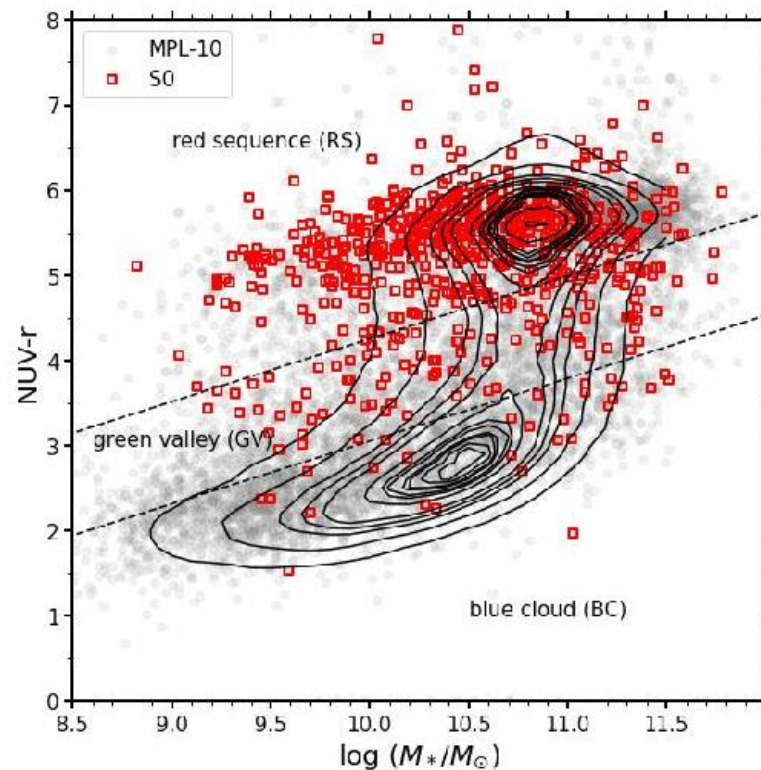


**Figure 3.**  $NUV - r$  versus  $M_*$  diagram. The black contours represent galaxies from the NSA catalogue. The grey circles and red squares are the MaNGA sample and S0 galaxies, respectively. Two dashed lines separate galaxies into blue cloud (BC), green valley (GV) and red sequence (RS).

# Больше 10% всех S0 имеют газ с рассогласованной кинематикой

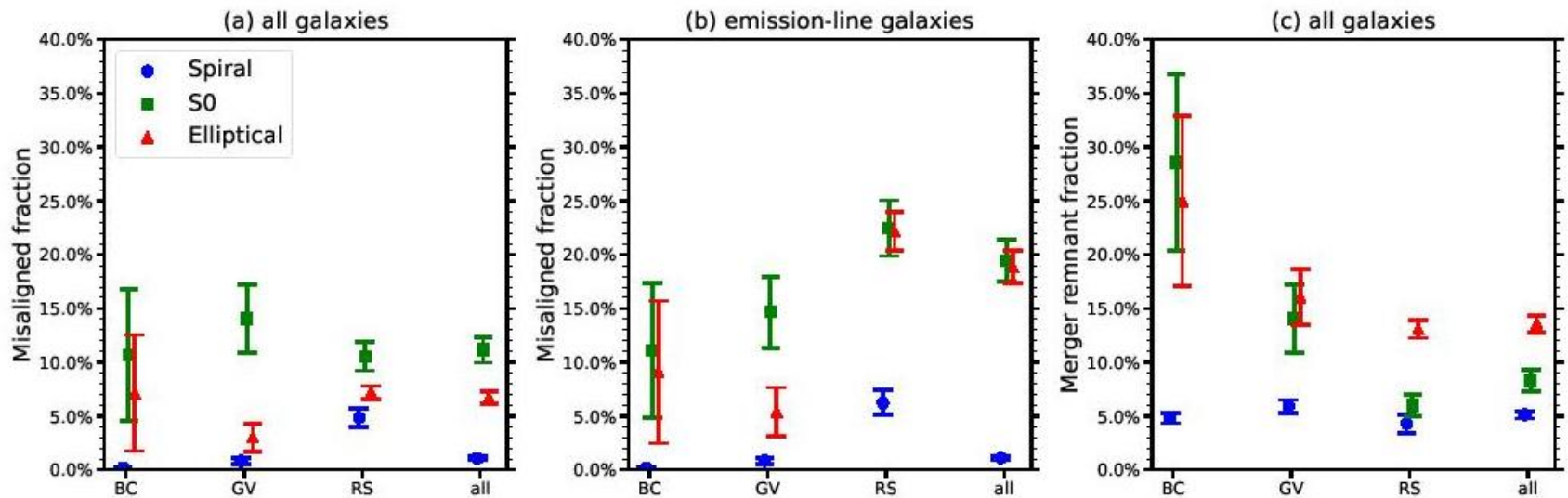


**Figure 4.** Panel (a) and (c) show the misaligned fraction and merger remnant fraction in the whole MaNGA sample, respectively. Panel (b) shows the misaligned fraction in the MaNGA emission-line galaxies sample. Blue circles are for spiral galaxies, green squares for S0 galaxies and red triangles for elliptical galaxies. Each morphological type is divided into BC, GV and RS. Each point in the same class (BC, GV, RS and all) is slightly offset in the  $x$ -axis to avoid overlap.

# Смотрим на левую картинку: это ОБЫЧНЫЕ S0, в отличие от мерждеров

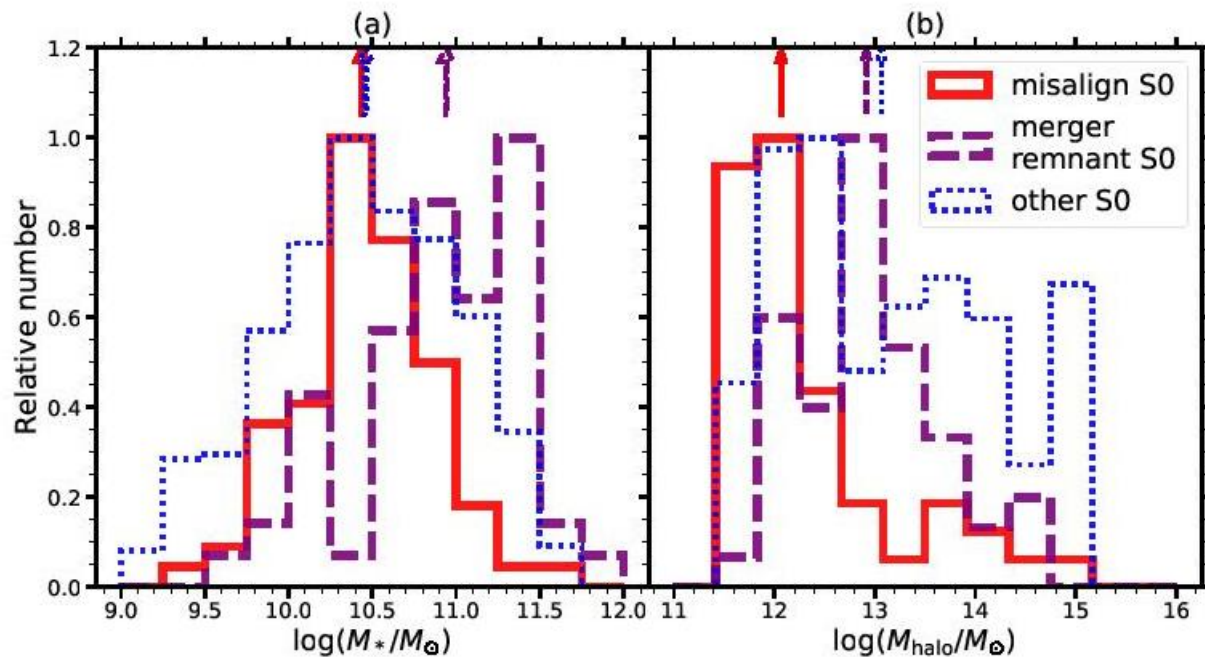


**Figure 5.** Panel (a) and (b) show the distribution of stellar mass  $M_*$  and dark matter halo mass  $M_{\text{halo}}$ , respectively. S0 galaxies are divided into galaxies with kinematic misalignments (red solid), merger remnants features (purple dashed) and others (blue dotted). The arrows at the top of each panel are the median of the distribution with the same color.

# Попытка поиска стимулированного звездообразования

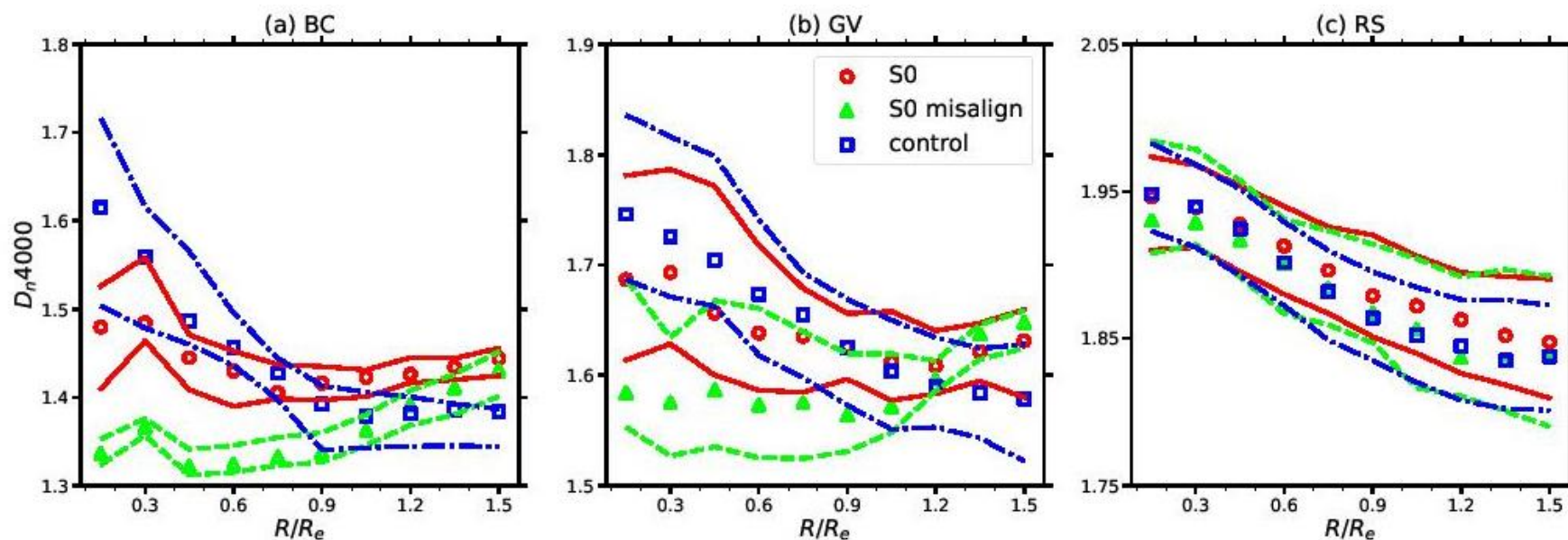


**Figure 6.** The  $D_n4000$  radial gradients for BC (left), GV (middle) and RS (right) misaligned S0 galaxies (green triangles), the whole S0 galaxies sample (red circles) and their control sample (blue squares). The dashed lines with the same color show the relevant 40 ~ 60 percentile range.

# ArXiv: 2303.04827

## Efficient Formation of Massive Galaxies at Cosmic Dawn by Feedback-Free Starbursts

Avishai Dekel<sup>1,2\*</sup>, Kartick C. Sarkar<sup>1,3</sup>, Yuval Birnboim<sup>1</sup>, Nir Mandelker<sup>1</sup>, Zhaozhou Li<sup>1</sup>

<sup>1</sup>*Racah Institute of Physics, The Hebrew University, Jerusalem 91904 Israel*

<sup>2</sup>*SCIPP, University of California, Santa Cruz, CA 95064, USA*

<sup>3</sup>*Astronomy, Tel Aviv University, Tel Aviv, Israel*

10 March 2023

### ABSTRACT

JWST observations reveal a surprising excess of luminous galaxies at  $z \sim 10$ , consistent with efficient conversion of the accreted gas into stars, unlike the suppression of star formation by feedback at later times. We show that the high densities and low metallicities at this epoch *guarantee* a high star-formation efficiency in the most massive dark-matter haloes. Feedback-free starbursts (FFBs) occur when the free-fall time is shorter than  $\sim 1$  Myr, below the time for low-metallicity massive stars to develop winds and supernovae. This corresponds to a characteristic density of  $\sim 3 \times 10^3 \text{ cm}^{-3}$ . A comparable threshold density permits a starburst by allowing cooling to star-forming temperatures in a free-fall time. The galaxies within  $\sim 10^{11} M_\odot$  haloes at  $z \sim 10$  are expected to have FFB densities. The halo masses allow efficient gas supply by cold streams in a halo crossing time  $\sim 80$  Myr. The FFBs gradually turn all the accreted gas into stars in clusters of  $\sim 10^{4-7.5} M_\odot$  within galaxies that are rotating discs or shells. The starbursting clouds are shielded against feedback from earlier stars. We predict high star-formation efficiency above thresholds in redshift and halo mass, where the density is  $10^{3-4} \text{ cm}^{-3}$ . The  $z \sim 10$  haloes of  $\sim 10^{10.8} M_\odot$  are predicted to host galaxies of  $\sim 10^{10} M_\odot$  with  $\text{SFR} \sim 65 M_\odot \text{ yr}^{-1}$  and sub-kpc sizes. The metallicity is  $\leq 0.1 Z_\odot$  with little gas, dust, outflows and hot circumgalactic gas, allowing a top-heavy IMF but not requiring it. The post-FFB evolution of compact galaxies with thousands of young clusters may have implications on black-hole growth and globular clusters at later times.



# Все ограничения сверху-снизу на тоненького, но проходят

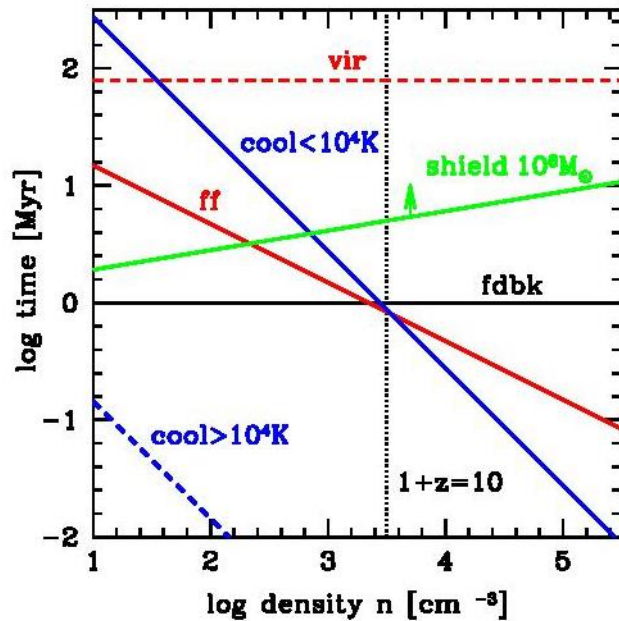


**Figure 3.** The timescales as a function of density. The feedback delay time  $t_{\text{fbk}} \sim 1$  Myr is from eq. (3). The free-fall time  $t_{\text{ff}}$  is from eq. (4). The cooling time at  $T < 10^4 \text{K}$   $t_{\text{cool}}$  is from eq. (9) with  $Z=0.02$  ( $\propto Z^{-1}$ ) and  $T = 10^4 \text{K}$ . The shielding time is the lower limit for the crushing time  $t_{\text{cc}}$  from eq. (15), for a clump of  $M_c = 10^6 M_\odot$  ( $t_{\text{cc}} \propto M_c^{1/3}$ ) and winds from a generation of  $M_{\text{gen}} = 10^9 M_\odot$  ( $t_{\text{cc}} \propto M_{\text{gen}}^{-1/2}$ ) in a volume of radius  $R_{\text{gal}} = 1$  kpc ( $t_{\text{cc}} \propto R_{\text{gal}}$ ). The virial time  $t_v$  is from eq. (23) at  $1+z=10$  ( $\propto (1+z)^{-3/2}$ ). We see that  $t_{\text{ff}}$  and  $t_{\text{cool}}$  are both comparable to  $t_{\text{fbk}} \sim 1$  Myr or shorter when the density is a few  $\times 10^3 \text{cm}^{-3}$  or larger. This defines the characteristic density and timescale for feedback-free starbursts. The atomic cooling time at  $T > 10^4 \text{K}$  being much shorter than  $t_{\text{vir}}$  and  $t_{\text{cc}}$  causes efficient cold inflow through the halo at

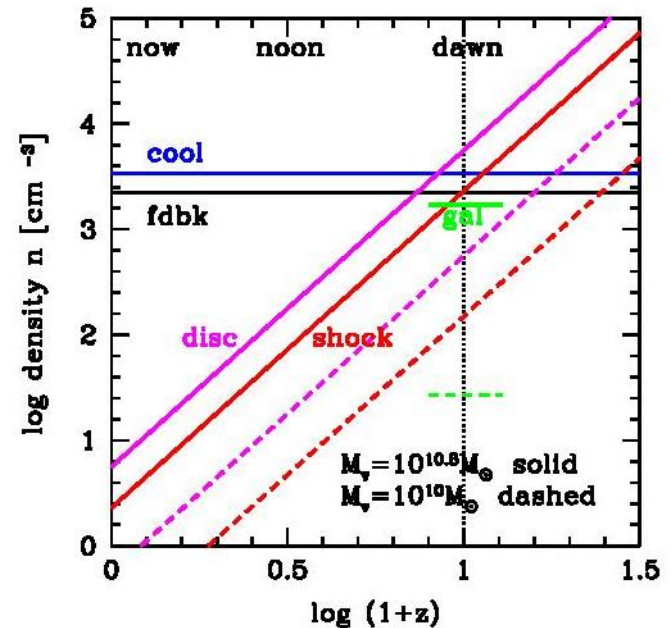


**Figure 4.** The gas densities  $n$  as a function of redshift for two values of halo virial mass. The feedback density  $n_{\text{fbk}}$  (where  $t_{\text{ff}} = t_{\text{fbk}}$ ) is from eq. (5) (where  $t_{\text{ff}} = t_{\text{fbk}}$ ). The cooling density  $n_{\text{cool}}$  (where  $t_{\text{cool}} = t_{\text{ff}}$ ) is from eq. (10) with  $Z=0.02$  and  $C=1$ . The post-shock density  $n_{\text{sh}}$  is from eq. (38) with  $R_{\text{vir}}=0.7$  kpc. The disc stellar density  $n_{\text{disc}}$  is from eq. (39) with  $\lambda=0.025$  and  $c=1$ . The observed galaxy density  $n_{\text{gal}}$  is from eq. (34) with  $R_e=0.3$  kpc and  $c=1$ . The actual densities in the star-forming clouds are a factor  $c > 1$  larger than the galaxy averages shown. Shown are the predictions for either  $M_v = 10^{10.8} M_\odot$  (solid) or  $M_v = 10^{10} M_\odot$  (dashed). In  $n_{\text{disc}}$  and  $n_{\text{gal}}$  the assumed efficiencies are  $\epsilon = 1$  and  $0.1$  for the two masses respectively. We see for  $M_v = 10^{10.8} M_\odot$  that at  $z \sim 10$  and above the densities  $n_{\text{disc}}$  and  $n_{\text{sh}}$ , as

# Схема формирования ранних галактик с особой эффективностью

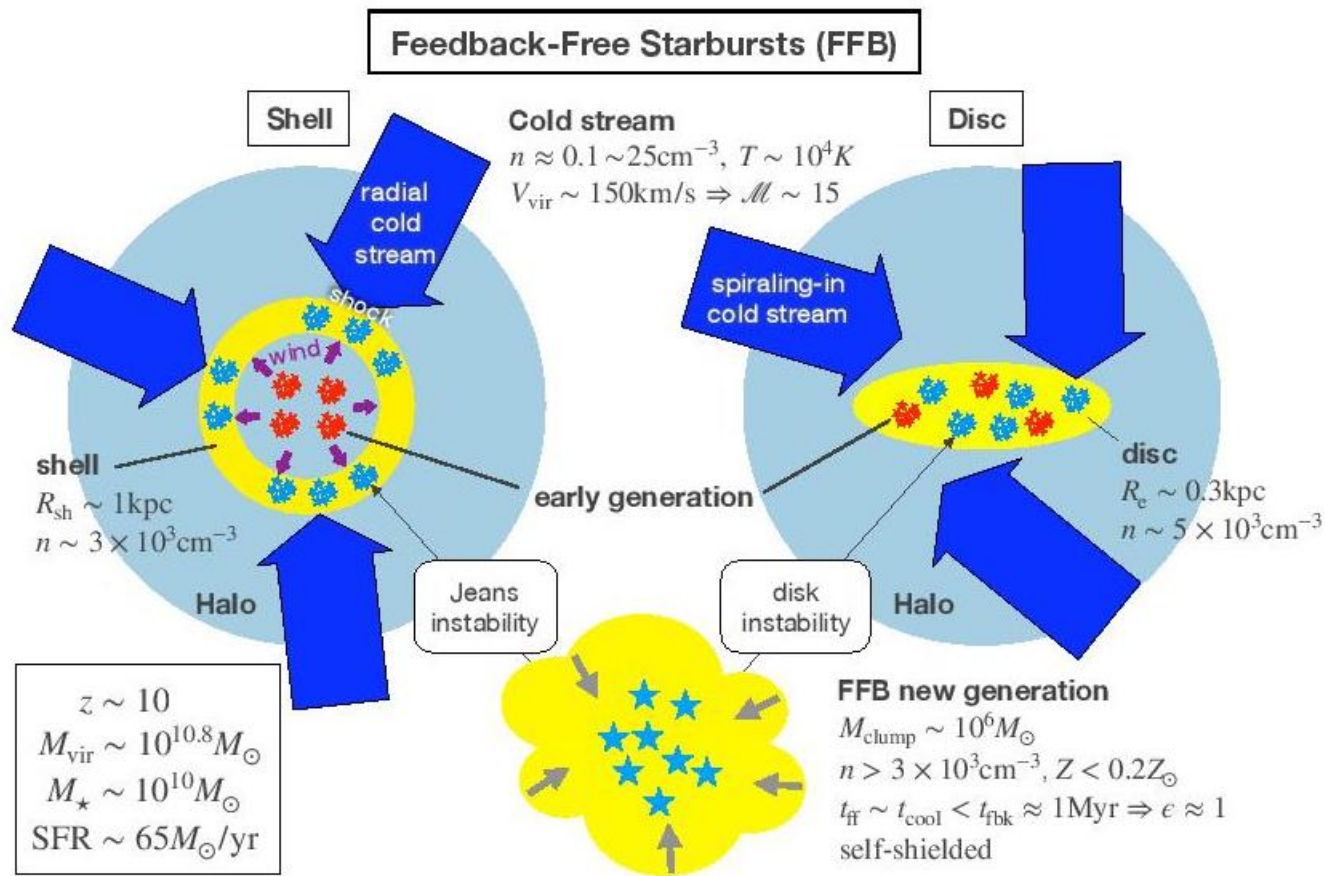


**Figure 5.** A cartoon illustrating a generation of feedback-free starbursts in massive clusters within a shell or a disc of  $n \sim 3 \times 10^3 \text{ cm}^{-3}$  at  $r \lesssim 1 \text{ kpc}$ . The shell is confined by the shock generated by the inflowing supersonic cold streams and by the wind from an earlier generation of stars, while the disc size is determined by angular momentum. Shell fragmentation is allowed after the gas accreted locally exceeds the Jeans mass, while the disc fragments after the accreted gas brings the Toomre  $Q$  to below unity. Starbursts follow in the clusters as  $t_{\text{cool}} < t_{\text{ff}}$ .

# Пока статистика невелика, стандартная $\Lambda$ CDM-модель еще СТОИТ...

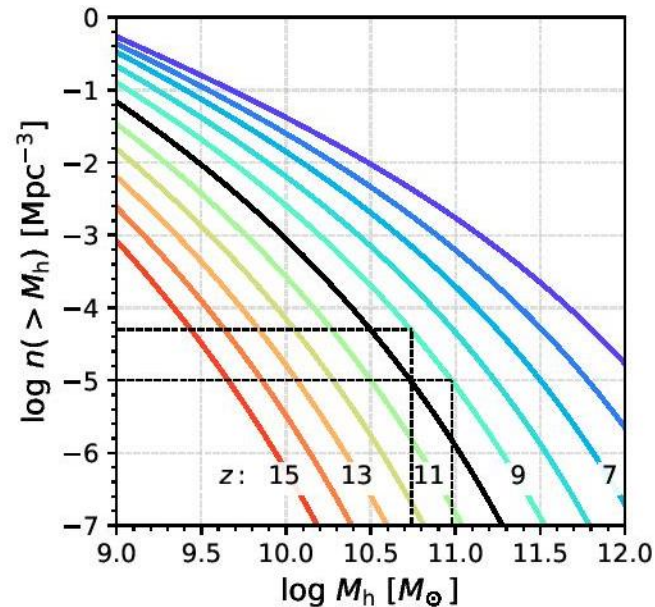


**Figure 6.** The cumulative halo mass function at different redshifts (Watson et al. 2013). It assumes a  $\Lambda$ CDM cosmology with  $\Omega_m = 0.3$ ,  $\Omega_\Lambda = 0.7$ ,  $h = 0.7$  and  $\sigma_8 = 0.82$ . The haloes are spherical with a mean density contrast of 200. This serves for estimating the halo masses of galaxies in a complete sample within a given effective volume, assuming rank-preserving abundance matching between the galaxy luminosities and the halo masses. With a volume of  $10^5 \text{ Mpc}^3$ , the halo mass of the brightest galaxy at  $z \approx 9$  is expected to be  $M_v \approx 10^{11} M_\odot$ , and the 5th brightest galaxy is expected to have  $M_v \sim 10^{10.8} M_\odot$ , as marked by the dashed lines.